Supplementary Figure 1

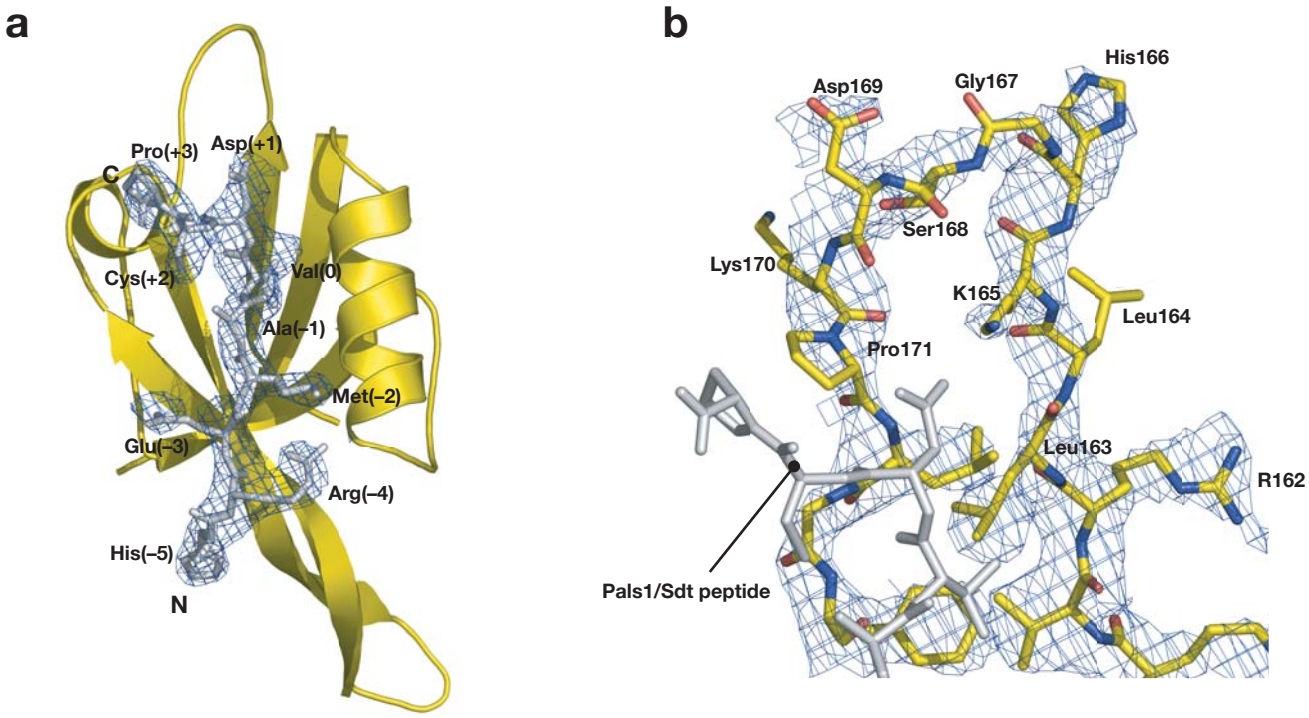

Supplementary Figure 1 Structure of the Par-6 PDZ in complex with the internal Pals1 ligand. (**a**) Ribbon representations of the Pals1 bound Par-6 PDZ domain. The Pals1 ligand is shown in grey with residues labeled and numbered according to standard PDZ nomenclature (residue zero would be the C-terminal residue). Electron density from a $2F_O$-F_C simulated annealing composite omit map contoured at 1σ is shown around the peptide. (**b**) The carboxylate-binding loop. Residues 162-171 from the Par-6 PDZ domain which connect the β1 and β2 strands of the Par-6 PDZ domain are shown in stick representation with electron density as in (a). A portion of the Pals1 ligand is shown for orientation.

Supplementary Figure 2

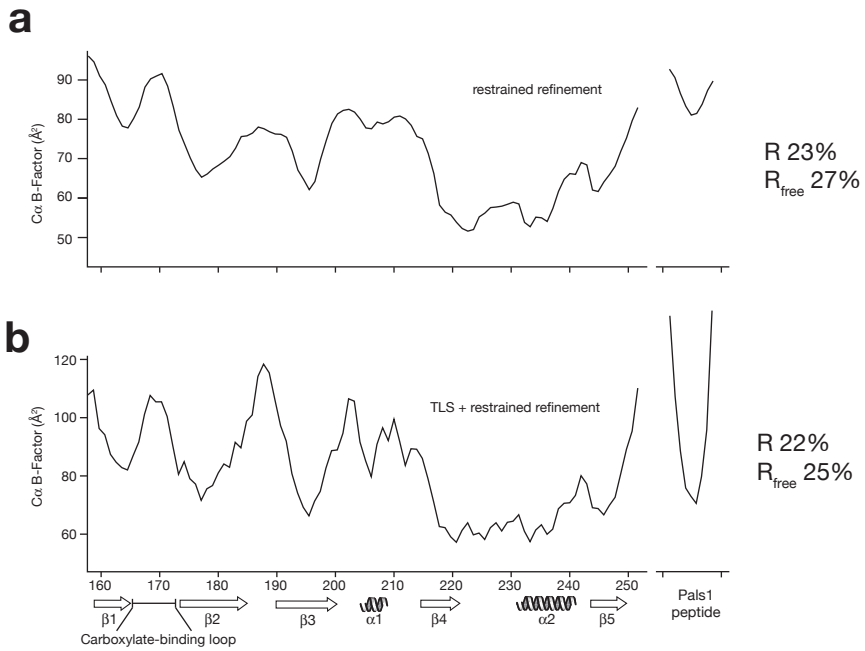

Supplementary Figure 2 B-factor analysis of the Par-6–Pals1 complex. (**a**) Plot of the alpha carbon isotropic B-factor as a function of residue after restrained refinement. (**b**) Plot of the alpha carbon isotropic B-factor as a function of residue after TLS (translation-libration-screw) and restrained refinement.

Supplementary Figure 3

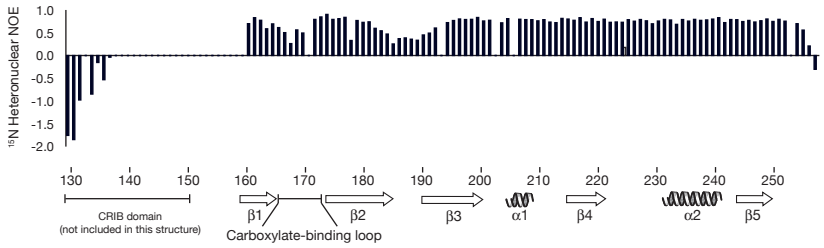

Supplementary Figure 3 Heteronuclear NOE analysis of the Par-6 CRIB-PDZ fragment bound to the Pals1 peptide. Values of zero are not measured (proline residues or residues that are not yet assigned). The Par-6 CRIB domain is unstructured as shown by its negative NOE values. Although the carboxylate binding loop is more dynamic than the core of the protein, it is still well-ordered.

Supplementary Figure 4

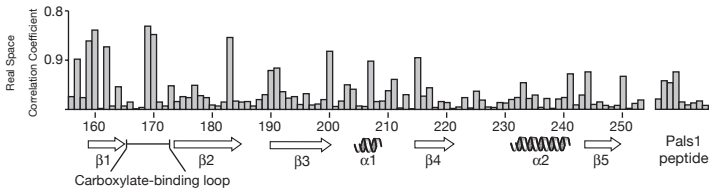

Supplementary Figure 4 Real space correlation coefficients as a function of residue for the refined model. No residue has a coefficient below 0.8 indicating that the model is well described by the electron density.